

Journal Pre-proofs

Environmentally superior cleaning of diatom frustules using sono-Fenton process: Facile fabrication of nanoporous silica with homogeneous morphology and controlled size

Peyman Gholami, Alireza Khataee, Amit Bhatnagar

PII: S1350-4177(19)31450-6

DOI: <https://doi.org/10.1016/j.ultsonch.2020.105044>

Reference: ULTSON 105044

To appear in: *Ultrasonics Sonochemistry*

Received Date: 12 September 2019

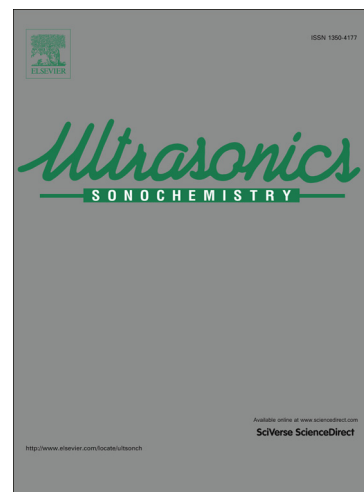
Revised Date: 28 January 2020

Accepted Date: 24 February 2020

Please cite this article as: P. Gholami, A. Khataee, A. Bhatnagar, Environmentally superior cleaning of diatom frustules using sono-Fenton process: Facile fabrication of nanoporous silica with homogeneous morphology and controlled size, *Ultrasonics Sonochemistry* (2020), doi: <https://doi.org/10.1016/j.ultsonch.2020.105044>

This is a PDF file of an article that has undergone enhancements after acceptance, such as the addition of a cover page and metadata, and formatting for readability, but it is not yet the definitive version of record. This version will undergo additional copyediting, typesetting and review before it is published in its final form, but we are providing this version to give early visibility of the article. Please note that, during the production process, errors may be discovered which could affect the content, and all legal disclaimers that apply to the journal pertain.

© 2020 Elsevier B.V. All rights reserved.



**Environmentally superior cleaning of diatom frustules using sono-Fenton
process: Facile fabrication of nanoporous silica with homogeneous
morphology and controlled size**

Peyman Gholami,^{a,b} Alireza Khataee,^{a,c,d,*} Amit Bhatnagar^b

^a Research Laboratory of Advanced Water and Wastewater Treatment Processes, Department of Applied Chemistry, Faculty of Chemistry, University of Tabriz, 51666-16471 Tabriz, Iran

^b Department of Environmental and Biological Sciences, University of Eastern Finland, P.O. Box 1627, FI-70211 Kuopio, Finland

^c Department of Materials Science and Nanotechnology Engineering, Faculty of Engineering, Near East University, 99138 Nicosia, TRNC, Mersin 10, Turkey

^d Institute of Research and Development, Duy Tan University, Da Nang 550000, Vietnam

* Corresponding author:

a_khataee@tabrizu.ac.ir

alirezakhataee@duytan.edu.vn

Abstract

Existing techniques for the preparation of silica structures from diatom cells include cleaning of frustules through baking at high temperature and oxidant cleaning using concentrated sulfuric acid, hydrogen peroxide, nitric acid, or sodium dodecyl sulfate (SDS)/ethylenediaminetetraacetic acid (EDTA). In this study, sono-Fenton (SF) process was examined to prepare nanoporous silica through cleaning diatom frustules, while preserving their structural features. Single colonies of *Cyclotella sp.* were cultivated in batch mode [f/2-enriched seawater](#). Combination of Fenton process with ultrasonication was found to be more efficient than the sum of individual processes in the removal of organic compounds from *Cyclotella sp.* structure. The optimized amounts of operational parameters were determined as suspension pH of 3, diatom cell density of 4.8×10^5 cell mL⁻¹, H₂O₂ concentration of 60 mM, Fe²⁺ concentration of 15 mM, ultrasound irradiation power of 400 W and the temperature of 45 °C. The results of energy-dispersive X-ray spectroscopy (EDX) and thermal gravimetry (TG) analyses proved that organic materials covering the cell wall were significantly removed from the frustules through SF process. Scanning electron microscopy (SEM) images showed that after SF treatment, silica nanostructures were produced having uniform pores less than 15 nm in diameter. N₂ adsorption-desorption isotherms demonstrated that almost non-porous structure of diatom frustules became mesoporous during removing the organic matrix. Lipids, amino acids, carbohydrates and organic acids or their oxidized products were identified using GC-MS analysis as the main organic compounds released from diatom cells to the solution after SF treatment. [Treated frustules exhibited adsorption capability of 91.2 mg/g for Methylene Blue, which was almost 2.5 times higher than that of untreated frustules \(34.8 mg/g\).](#)

Keywords: Silica nanostructures; Cleaning of diatom cells; Sono-Fenton; Frustules; *Cyclotella sp.*

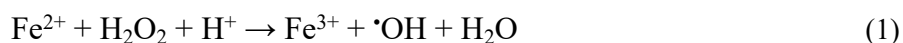
1. Introduction

Nature shows extraordinary complex architecture in different microorganisms and this is why material scientists derive innovation in designing novel biomaterials using these structures [1]. Diatoms, as one of the examples of such microorganisms, has attracted considerable attention owing to their unique architecture of cell walls (frustules), which is related to their excellent photosynthesis performance [2]. They are found in the waterways, oceans, soils and produce approximately 20% of the oxygen generated on the earth annually [3]. Diatoms are generally known as fast-growing and dominant species (about 50%) of phytoplankton community under unlimited condition, given enough silicate and nutrients content higher than approximately $2 \mu\text{mol L}^{-1}$ silicate [4, 5]. Based on differences in morphology and structure of the frustules, more than 100,000 various diatoms species are classified [5]. Gordon and Drum, for the first time, proposed the potential application of diatom frustules in nanotechnology in 1994 [6]. Since then, considerable attention has been paid to the capability of unicellular diatoms to synthesize three-dimensional silica with a specific structure [5, 7]. According to the literature, the diatoms frustules have been characterized by their biocompatibility, multiple pore surfaces, excellently ordered micro/nanostructures, unique optical characteristics, mechanical and thermal stability and have been considered as potential candidates for different applications [8, 9]. Particularly, frustules can act as photonic crystals owing to the shape and size of pore morphology bodies, which leads to unique optical characteristics [10]. Incorporation of some biomolecules such as antibodies, enzymes and proteins into the individual structure of frustule can result in the development of hybrid bioreactor and biosensor that provides new opportunities in nanomedicine and biotechnology fields [11, 12]. Several research works have been conducted to study the application of frustules in solar cells, instead of the high-cost sensitized TiO_2 [13]. Because of biological

compatibility, chemical inertness and porous structure, the frustules possess the promising potential to be applied as a drug delivery carrier [14]. The other interesting applications of diatoms include catalysis, adsorption, efficient filtration, immunoprecipitation and nanofabrication without altering the 3D structure which can provide the novel strategies in nanotechnology [8, 9, 15, 16]. The cell wall of the diatom is covered by an organic matrix that protects the frustule from dissolution in the aqueous medium. For most applications, the organic materials embedding the cell wall should be eliminated [17, 18]. Sulfuric acid, hydrogen peroxide, nitric acid, or sodium dodecyl sulfate (SDS)/ethylenediaminetetraacetic acid (EDTA) oxidants are most frequently proposed for removal of the organic components [19-21]. In the conventional cleaning processes using above-mentioned reagents, the concentrated and hot acidic solution is used for a certain period of time. However, the obtained acidic solution could not be removed using filter cloths due to its corrosive and oxidizing behavior. On the other hand, the subsequent dilution or centrifugation may take several hours to remove acidic solution. For instance, collection of frustules from 1000 mL diatom suspension (cultivated for 14-21 days) requires almost 600 mL of 98% sulfuric acid and produces 2-4 L of waste liquid [21]. Moreover, the organic compounds are not completely eliminated due to agglomeration of the cells and insufficient contact between the organic matrix and oxidant [21]. High temperature (500-900 °C) baking is also conducted to eliminate the organic matrix from diatom frustules, but may damage the cribellum [22]. Therefore, the conventional frustule cleaning processes need to be improved to produce large quantities of high-quality frustules for different applications.

Fenton process as one of the advanced oxidation processes (AOPs) uses the reaction between ferrous ions and hydrogen peroxide to produce $\cdot\text{OH}$ radicals (Eq. 1), which can non-selectively oxidize most organic compounds [23]. Sonolysis is another AOP method which can produce $\cdot\text{OH}$

radicals through water dissociation as a result of generation of local fields, known as hot spots, with the high temperature and pressure (Eq. 2) [24]. Recently, great attentions have been paid on the combination of Fenton process and ultrasonic irradiation as a new AOP, which is known as sono-Fenton (SF) process. Promising studies have been performed in the removal of different organic contaminants including dyes, pharmaceutical compounds and pesticides using SF process [25, 26].



SF process can provide sufficient potential for the removal of organic compounds from diatom cells through additional production of reactive radical species. Moreover, utilization of ultrasonic irradiation during the cleaning process can remarkably inhibit the agglomeration of the cells, which can lead to the production of high-quality frustules. To the best of our knowledge, this is the first study that reports the removal of organic materials covering diatom cells using SF process. The aims of this study are: (a) to examine the ability of sono-Fenton process in cleaning of diatom frustules, (b) to investigate the effect of operational parameters such as concentration of Fe^{2+} and H_2O_2 , suspension pH, the ultrasound power, the cell density of diatom and temperature on removal of total organic carbon (TOC) and total nitrogen (TN) from diatom cells, (c) and to characterize the properties and structure of diatom frustules before and after performing sono-Fenton process using X-ray diffraction (XRD), scanning electron microscopy (SEM), energy-dispersive X-ray spectroscopy (EDX), Fourier transform infrared spectroscopy (FT-IR), N_2 adsorption-desorption process and thermal gravimetry (TG) analyses. Finally, the organic materials released from the diatom cells were identified using gas chromatography-mass spectroscopy (GC-MS).

2. Experimental

2.1. Materials and methods

Cyclotella sp. cells were obtained from the Iranian Biological Resource Center. H₂O₂ (30%), FeSO₄·4H₂O (99%), NaOH (≥ 98%), H₂SO₄ (≥ 98%), HCl (37%), diethyl ether (C₄H₁₀O, ≥99.7%), ammonium formate (HCO₂NH₄, 99.9%), N,O-bis-(trimethylsilyl)-acetamide (C₈H₂₁NOSi₂, ≥95%), and Methylene Blue (C₁₆H₁₈N₃SCl) were purchased from Merck (Germany).

2.2. Cultivation of *Cyclotella sp.*

Cultivation of single colonies of *Cyclotella sp.* was carried out in batch mode f/2-enriched seawater at 18 ± 1 °C and pH 7, under a light intensity of 70 μmol m⁻² s⁻¹. Typically, the cultivation was performed as follows: (i) The growth of *Cyclotella sp.* in 100 mL Erlenmeyer flask containing 50 mL culture medium with cell density of 3.0 × 10⁴ cells mL⁻¹ (7 days), (ii) dilution of obtained inoculums for three times using fresh f/2-enriched seawater at volume ratios of 1:10, 1:10 and 1:4 and performing the successive cultivations for 7, 7 and 14 days intervals, respectively. The final cell density was determined using a microscope (Olympus CH-2) and a Sedgwick rafter chamber (Pysen- SGI Ltd. UK) as 8.2 × 10⁶ cells mL⁻¹. Finally, the grown *Cyclotella sp.* cells were harvested by centrifugation at 4000 rpm for 15 min and washed three times with deionized water.

2.3. Cleaning diatom frustules using sono-Fenton process

Each sono-Fenton run was conducted as follows. A certain amount of the Fenton agents (Fe²⁺ and H₂O₂) was added to 80 mL algae suspension (2 × 10⁶ – 8 × 10⁶ cells mL⁻¹). Then, the suspension pH was adjusted at a certain value and the reaction vessel was sonicated using an EP

S3 Sonica ultrasonic bath (Italy) with a constant frequency of 40 kHz. During the reaction, the reactor was fixed at the center of ultrasonication bath and the distance between them was kept constant at 1.0 cm to provide the same conditions for all the experiments. After 4 h ultrasound irradiation, 30 mL treated suspension was collected by centrifuging at 4000 rpm for 15 min, and washed for two times with ammonium formate (0.5 M) and deionized water and dried at 10 °C for 24 h. Then, the performance of SF process in removing organic matrix from diatom frustules was evaluated by determining total organic carbon (TOC) and total nitrogen (TN) removal efficiencies (RE%) based on (Eqs. 3 and 4), respectively.

$$\text{TOC RE\%} = \frac{\text{TOC}_i - \text{TOC}_f}{\text{TOC}_i} \times 100 \quad (3)$$

$$\text{TN RE\%} = \frac{\text{TN}_i - \text{TN}_f}{\text{TN}_i} \times 100 \quad (4)$$

where TOC_i and TOC_f are the initial and final TOC, and TN_i and TN_f denoted as initial and final TN value of the samples, respectively.

2.4. Characterization

The XRD patterns of untreated frustules (UF) and treated frustules (TF) were determined using Bruker AXS D8 advance diffractometer with Cu Ka radiation ($\lambda = 0.15418$ nm) to investigate the crystal structure of the samples. SEM images were obtained using Zeiss sigma HDVP (Carl Zeiss GmbH, Germany) microscope equipped with an EDX analyzer. FT-IR spectroscopy was conducted on a Tensor 27 FT-IR spectrometer (Bruker, Germany). TGA analysis was carried out up to 1000 °C at a rate of 10 °C/min using a TGA Q600 (TA Instruments, USA). N₂ adsorption-

desorption analysis was carried out using a TriStar (Micromeritics Instrument Corp. Norcross, GA, USA) at 77 K.

2.5. Determination of the degradation intermediates

GC–MS was used to detect the organic materials, released from diatom cell to the solution during SF process. After 240 min of SF treatment under the optimized experimental conditions, the treated diatom frustules were removed from the solution by centrifuging. Then, the solution was mixed with 20 mL diethyl ether three times to extract the organic materials from the aqueous phase to the organic phase. The organic phase was evaporated and then dissolved in 100 μL of N,O-bis-(trimethylsilyl)-acetamide followed by 20 min stirring at 60°C. Subsequently, in order to identify the existing organic compounds, the obtained solution was analyzed by an Agilent 6890 gas chromatograph equipped with an Agilent 5973 mass spectrometer (Agilent, CA, USA) using an HP-5MS column (0.25 μm film thickness, 30 m \times 0.25 mm) by the method described in our previous work [27].

2.6. Adsorption tests

Adsorption tests were performed in a batch reactor to investigate Methylene Blue (MB) removal from aqueous solution using UF and TF. Working solutions with MB concentration of 50 mg L^{-1} were prepared by diluting MB stock solution (500 mg L^{-1}) with milli Q water. A certain amount of the adsorbent was mixed with MB solution (40 mL, 50 mg L^{-1}) in the polyethylene falcon tube at pH 5.6 (the natural pH) under ambient conditions. The suspension was shaken at 220 rpm to reach equilibrium. The treated MB solutions were separated from the adsorbent through filtration by a 0.45 μm membrane syringe filter. The concentration of the unadsorbed MB left behind in each solution was determined using a Shimadzu UV-1700 UV–vis spectrophotometer at

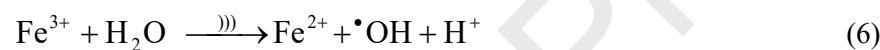
the λ_{\max} of 665 nm. The equilibrium capacity (q_e) (mg/g) of the adsorbents for MB removal was determined using the following equation: $q_e = \frac{(C_i - C_e)V}{m}$, where V is referred to the solution volume (L), m is the adsorbent weight (g), C_i , and C_e are the initial and equilibrium concentrations (mg L^{-1}) of MB, respectively.

3. Results and discussion

3.1. Comparison of different processes for the removal of organic materials from diatom frustules

Fig. 1 (a) shows a comparative investigation on the cleaning of diatom frustules by means of total organic carbon (TOC) and total nitrogen (TN) removal efficiencies (RE%) using different processes. Low TOC (6.9%) and TN (4.3%) removal efficiencies were observed when diatom suspension was subjected to H_2O_2 oxidant. To investigate the cleaning ability of mechanical stirring, the diatom suspension was vigorously stirred (2000 rpm) without adding H_2O_2 and Fe^{2+} . The observations demonstrated that the mechanical stirring also could not effectively remove the organic matrix from diatom cells (TOC RE% = 7.5% and TN RE% = 9.4%). However, when H_2O_2 was employed along with Fe^{2+} , TOC and TN removal efficiencies were reached to 41.5% and 43.8%, respectively. The reason for higher TOC and TN removal efficiencies is the high generation of reactive oxygen species (ROS) in $\text{H}_2\text{O}_2/\text{Fe}^{2+}$ process which are stronger oxidants than H_2O_2 . Moreover, 28.7% TOC and 23.3% TN removal efficiencies were obtained when the suspension was exposed to ultrasound irradiation (US alone). The highest TOC (91.6%) and TN (87.4%) removal efficiencies were achieved through SF process. Ultrasonication is the feasible method for water molecules dissociation (Eq. 2) and Fe^{2+} regeneration in Fenton process (Eqs. (5) and (6))

resulting in the formation of extra reactive species in the suspension [28]. Moreover, **ultrasonication** generates different physical effects in an aqueous phase. Ultrasound irradiation creates a high-turbulence condition leading to a steady flow away from the piezo location, which is recompensed with inflows from the sides. Owing to the opposite direction movements in the liquid phase, the acoustic flow effect is formed which is followed by remarkable mass transfer [29]. Moreover, microbubble flow is created in an acoustic environment because of the interactions between gas microbubbles and ultrasound waves. In addition, two additional forces including shockwaves and microjets are produced during acoustic cavitation. When the cavitation microbubbles collapse symmetrically, high intensity shock waves are produced and when they collapse asymmetrically, high intensity microjets are produced [29, 30].



In order to further compare the **performances** of the different systems, synergy factors for TOC and TN removal efficiencies (TOC RE% synergy factor_{SF} and TN RE% synergy factor_{SF}) were determined as 1.4 and 1.3 (Eqs. (7 and 8)). A synergy factor of 1.0 shows additive repression, whereas a value higher than 1 represents synergy.

$$\text{TOC RE\% synergy factor}_{SF} = \frac{\text{TOC RE\%}_{SF}}{\text{TOC RE\%}_{US} + \text{TOC RE\%}_{Fenton}} \quad (7)$$

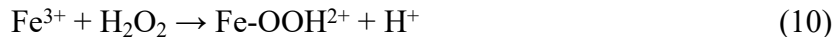
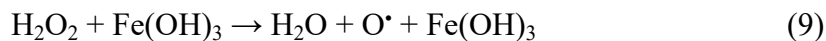
$$\text{TN RE\% synergy factor}_{SF} = \frac{\text{TN RE\%}_{SF}}{\text{TN RE\%}_{US} + \text{TN RE\%}_{Fenton}} \quad (8)$$

A series of scavenging experiments were conducted for detection of the main reactive species for removal of organic materials from diatom frustules. 1,4-Benzoquinone (BQ) and isopropanol (IPA) were selected as the scavengers of $\text{HO}_2^\bullet/\text{O}_2^{\bullet-}$ and $^\bullet\text{OH}$ radicals, respectively [27, 31]. As shown in Fig. 1 (b), removal of organic materials through US, Fenton and SF processes was considerably affected by both BQ (0.2 M) and IPA (0.2 M). Nevertheless, the addition of IPA caused a higher quenching effect than that of BQ, revealing that $^\bullet\text{OH}$ was the major oxidizing agent responsible for cleaning of diatom frustules.

<Fig. 1>

3.2. Effect of operational parameters

In order to evaluate the effect of suspension pH on the removal of organic materials from the diatom cell wall, the pH of diatom suspension was adjusted to 3, 5, 7, and 9 with H_2SO_4 and NaOH (0.1 M) before ultrasonication. As can be seen from Fig. 2 (a), when suspension pH was adjusted to 3, maximum TOC (67.7%) and TN (60.4%) removal efficiencies were observed in SF process. The performance of SF process decreased at pH higher than 3, which could be due to the Fe^{3+} ions precipitation via the available OH^- ions. $\text{Fe}(\text{OH})_3$ could dissociate H_2O_2 into water and oxygen (Eq. (9)), and as a consequence, the removal efficiency decreased because of the generation of a low amount of ROS. Furthermore, at pH values higher than 5, Fe^{2+} complexation as $[\text{Fe}(\text{II})(\text{H}_2\text{O})_6]^{2+}$ was formed that reacts with H_2O_2 more slowly than $[\text{Fe}(\text{II})(\text{OH})(\text{H}_2\text{O})_5]^{2+}$ and hence, produces a lower concentration of ROS. These effects were reversed at acidic conditions, as the excess H^+ ions accelerate the backward reaction (Eq. (10)) causing an increment in concentration of Fe^{3+} .



On the other hand, the redox potential of $\bullet\text{OH}$ radicals increases at the acidic condition. The oxidation potential for the redox couple $\bullet\text{OH}/\text{H}_2\text{O}$ has been reported to be 2.59 V vs. normal hydrogen electrode (NHE) at pH 0 and 1.64 V vs. NHE at pH 14 [28]. A similar result has been reported by Tantak and Chaudhari for the decolorization of Reactive Black 5 solution by the Fenton reaction [32]. In this work, both TOC and TN RE% decreased by increasing the pH value from 3 to 9.

Since H_2O_2 is a source of $\bullet\text{OH}$ radicals, the initial concentration of H_2O_2 has an important influence on the performance of SF system. The effect of initial concentration of H_2O_2 (20-50 mM) on TOC and TN removal efficiencies was examined at a constant Fe^{2+} concentration of 5 mM and pH 3. The observed results after the reaction time of 240 min are presented in Fig. 2 (b). The increment in the concentration of H_2O_2 enhanced the removal of organic materials from diatom frustules due to the improvement in the production of $\bullet\text{OH}$ radicals. The maximum TOC and TN removal efficiencies of 83.6% and 71.1% were observed for SF process using 60 mM of H_2O_2 . Nevertheless, H_2O_2 overdose in the diatom suspension has an inhibition effect on the performance of SF process by scavenging $\bullet\text{OH}$ radicals through Eq. (11) [28].

In the conventional H_2O_2 cleaning method, diatom cells are introduced to a solution containing 12.8 M H_2O_2 and 12.9 M HCl and stirred (≤ 200 rpm) at 90 °C for 24 h [20]. In fact, the amount of H_2O_2 consumption and reaction time in this study were almost 215 and 6 times lower than those in the conventional cleaning method. In addition, HCl consumption in SF process is negligible compared to the method used in previous studies [20].



The influence of Fe^{2+} concentration (5–35 mM) on the performance of SF process in the cleaning of diatom frustules is presented in Fig. 2 (c). As can be seen from Fig. 2 (c), an increase in Fe^{2+} concentration from 5 to 15 mM increased the TOC and TN removal efficiencies, but the further increment in Fe^{2+} (from 15 to 35 mM) led to a slight decrease in the performance of the process. The improving trend is owing to the fact that higher concentration of Fe^{2+} can produce more $\cdot\text{OH}$ radicals via Fenton reaction (Eq. (1)), hence resulting in higher removal of organic materials from the diatom cell wall. Afterward, a vice versa trend is observed, and the TOC and TN removal efficiencies decreased. The reason of this observation is that the excessive Fe^{2+} ions decrease the removal of organic materials to the competitive consumption of $\cdot\text{OH}$ radicals through (Eq. 12) [33]:



Since the amount of target organic materials exposed to the oxidation is an important parameter, the influence of cell density ($4.8 \times 10^5 - 7.2 \times 10^5$ cell mL^{-1}) was studied on the efficiency of SF process. As it can be observed in Fig. 2 (d), TOC and TN removal efficiencies were inversely proportional to diatom density in the suspension, which is owing to the availability of constant dosage of ROS irrespective of a large number of organic materials [34]. Consequently, the performance of the system decreased with increasing cell density from 4.8×10^5 cell mL^{-1} to 7.2×10^5 cell mL^{-1} .

In order to study the temperature effect on the cleaning of diatom frustules through SF process, a number of experiments were carried out by varying the reactor temperature from 15 to 45 °C under the optimized amounts of other parameters. The TOC and TN removal efficiencies at various temperatures are shown in Fig. 2 (f). The obtained results demonstrated that the increment of the temperature from 15 to 45 has a favorable influence on the performance of SF process. Generally, the production of ROS like $\cdot\text{OH}$ radicals is accelerated by increasing the solution temperature. Since the rate of Fenton reaction is enhanced by raising the temperature, superior TOC and TN removal efficiencies were observed at higher temperatures [31]. The optimized temperature in this study (45 °C) is two times lower than that in the conventional cleaning method (90 °C) [20].

<Fig. 2>

3.3. Characterization of untreated frustules (UF) and treated frustules (TF)

The morphologies of the UF and TF were characterized using SEM analysis. Fig. 3 (a and b) shows the SEM images of *Cyclotella sp.* cells grown in f/2-enriched seawater before SF treatment. The untreated *Cyclotella sp.* cells had a disk-like structure with a radius of $\sim 7 \mu\text{m}$ which are surrounded by some impurities. As can be seen from Fig. 3 (c and d), after treating the diatom cells using SF process, not only the impurities were eliminated, but the organic materials covering the cell wall were also removed from the frustules. Although SF treatment did not change the disk-like structure of *Cyclotella sp.* cells, the resulting frustules had clean surfaces, possessing uniform pores with a radius size of less than 15 nm. The results obtained from SEM images are in good agreement with those from N_2 adsorption-desorption analysis. EDX analysis was further employed to study the elemental composition of the samples. The EDX spectra of the UF and TF, along with

quantitative results, are shown in Fig. 3 (e and f), respectively. The quantitative results demonstrated that UF contains C, O, Si and Ca elements with weight percent (wt.%) of 52.67, 27.14, 16.69 and 3.50%, respectively. According to Fig. 3 (f), after SF treatment, the wt.% of C element significantly decreased from 52.67% to 7.23% and W% of Si increased from 16.69% to 42.93%. This can be attributed to the removal of the organic matrix from the surface of frustules.

<Fig. 3>

The XRD analysis was carried out to identify the phases of the samples. As can be seen from Fig. 4 (a), XRD patterns of UF and TF do not show any sharp peak, thereby revealing the amorphous nature of the samples. A broad peak at 2θ diffraction angle ranging from 13° to 30° demonstrates the presence of amorphous silica [35]. This kind of XRD pattern could be observed for many common minerals such as silica gel [36], opal-A [37], and diatoms [38] which contain amorphous silica.

FT-IR spectroscopy was conducted to determine the variations in surface functional groups of the diatom cells during SF process. Fig. 4 (b) shows the FT-IR spectra of UF and TF. In both curves, the peaks at 464 and 680 cm^{-1} are ascribed to Si–O and Si–O–Si stretching vibrations, respectively [39]. The vibration peaks appearing at 885 , 1040 , 1470 , 1514 , 1651 , and 1708 cm^{-1} are due to stretching vibrations of C–C [40], vibration C–O [27], cleavage of the C–N bonds [41], C=C stretching vibration of the aromatic skeleton [42], C=O stretching vibration [43], and vibration of –COOH [44], respectively. O–H stretching of surface-bound hydroxyl groups appeared at 3440 cm^{-1} [45]. In addition, two weak peaks at 2891 and 2947 cm^{-1} appeared which are attributed to symmetric and asymmetric stretching modes of C–H, respectively [46]. The

obtained results showed that although all the peaks in both spectra match well with each other in terms of position, some differences are clear in their intensity. The relative intensities of Si–O and Si–O–Si stretching vibrations in TF are higher than those in UF; on the contrary, the intensities of some other peaks (such as C–N and C–H) in TF are lower than those in UF which can be ascribed to removal of organic materials from the frustules during SF process.

Fig. 4 (c) shows the N₂ adsorption-desorption isotherms of UF and TF. According to Union of Pure and Applied Chemistry (IUPAC) classification, the isotherm of UF is Type II with H3 hysteresis loop extending till P/P₀ of 0.35. The isotherm type II is characteristic of almost non-porous materials. Its H3 hysteresis loop which does not show any limiting adsorption at high P/P₀ is assigned to assemblages of slit-shaped pores [47]. However, TF exhibits type IV isotherm with relatively narrow hysteresis loop of H1 type at high relative pressures, representing the existence of mesoporous structure with highly uniform cylindrical pores [47]. Accordingly, Brunauer–Emmett–Teller (BET) specific surface area and pore volume were significantly increased from 14.71 m² g⁻¹ and 0.022 cm³ g⁻¹ to 132.67 m² g⁻¹ and 0.18 cm³ g⁻¹, respectively.

The results of TGA demonstrated that after SF treatment, the organic compounds attached to the frustules were significantly removed from *Cyclotella sp.* cell wall. Fig. 4 (d) exhibits the weight loss of untreated and treated diatom samples as a function of temperature. In both samples, the first weight loss at temperature 35-120 °C is related to adsorbed water evaporation [48]. Almost 13% and 8% weight loss was obtained due to the release of adsorbed water in UF and TF, respectively. The main part of the weight loss of UF (around 49%) occurred at temperatures ranging from 200 to 400 °C which can be attributed to the loss of organic fraction [49]. However, the inconsiderable decrease (approximately 4%) was observed in TF weight at the same temperature range, which proves that silica is responsible for approximately 38% of *Cyclotella sp.*

cell weight. A diatom silica content of approximately 30-50 wt.% has been already reported in the literature [49, 50]. The results of TGA analysis are in good accordance with those obtained from EDX analysis.

<Fig. 4>

3.4. Identification of organic compounds released from diatom frustules

The organic compounds released from the diatom cell wall to the solution after SF treatment were detected using GC-MS. The obtained results including the name and structure of the compounds as well as the main fragments and retention times are presented in Table 1. GC-MS spectra of the identified organic compounds are also shown in Fig. S1. After treating the diatom suspension through SF process, these organic compounds could release from *Cyclotella sp.* cells into the suspension, which led to a decrease in the carbon content of TF (Fig. 3 (f)). This resulted in the accumulation of these compounds in the treated solution. As can be seen from Table 1, the identified compounds belong to lipids, amino acids, carbohydrates and organic acids or their oxidized products. Based on the literature review, all of these compounds are the main components of the organic content of the diatom cell [45]. Accordingly, the results obtained from both EDX and GC-MS analyses verified that SF system is an efficient technique for the removal of the organic materials from diatom cells.

<Table 1>

3.5. Adsorption of MB on UF and TF

Fig. 5 (a) displays the adsorption capacity of UF and TF for removal of MB from aqueous solution. The fast removal of MB using both adsorbents can be seen in Fig. 5; 88.6% and 95.7% of adsorption capacities were observed within 30 min for UF and TF respectively, because of the presence of many unoccupied sites for the MB molecules on the surface of adsorbents. No considerable variations were found in the adsorption capacities after 50 min; it means that the adsorption equilibrium time of both UF and TF is 50 min. The adsorption capability of TF was measured to be 91.2 mg/g, which was almost 2.5 times higher than that of UF (34.8 mg/g). The remarkable enhancement in adsorption capability of the TF revealed that the surface of diatom frustules was successfully cleaned through SF process. The higher performance of TF for MB removal can be ascribed to its mesoporous structure and larger specific surface area, which not only provide large interface and huge space for accommodation of guest species, but also enhance the mass transfer coefficient [51, 52].

<Fig. 5>

4. Conclusions

A comparative investigation on the cleaning of diatom frustules using different processes including Fenton, ultrasound and sono-Fenton systems has been conducted by means of determination of total organic carbon and total nitrogen removal efficiencies. Combining Fenton process with ultrasonication exhibited a positive synergy, in terms of TOC and TN removal efficiencies, while the addition of hydrogen peroxide alone to the diatom suspension had no remarkable beneficial influence. The results indicated that the highest TOC (91.6%) and TN (87.4%) removal efficiencies were achieved through sono-Fenton process. Increasing the

temperature and ultrasonic power caused the enhanced removal of the organic matrix from diatom structure through SF process. Conversely, increasing the pH of suspension and diatom density led to decreased removal efficiency. Moreover, the performance of SF process enhanced with increasing Fe^{2+} and H_2O_2 concentrations up to 15 and 60 mM respectively, but further increase resulted in a slight decrease in the efficiency of the sono-Fenton process. SEM images revealed that although SF treatment made no change in the disk-like shape of *Cyclotella sp.* cells, the treated sample had clean frustules with uniform and homogeneous pores with a radius size of less than 15 nm. The results of EDX and TGA analyses demonstrated that the weight percent of C element significantly decreased and the weight percent of Si increased during sono-Fenton process. GC-MS analysis verified the existence of lipids, amino acids, carbohydrate and organic acids or their oxidized products in the treated solution which are commonly attached to the cell structure of diatoms. SF treated diatom sample displayed a higher adsorption capacity than untreated diatom for MB because of its mesoporous structure and larger specific surface area. Sono-Fenton process can be introduced as a suitable method for the production of nanoporous silica from diatom frustules that is both cost-effective and environmentally benign.

Acknowledgements

The authors acknowledge the support provided by the University of Tabriz. P. Gholami would like to thank Centre for International Mobility (CIMO), Finland for providing EDUFI fellowship (decision number TM-18-10895).

References

- [1] N. Groen, M. Guvendiren, H. Rabitz, W.J. Welsh, J. Kohn, J. de Boer, Stepping into the omics era: Opportunities and challenges for biomaterials science and engineering, *Acta Biomaterialia*, 34 (2016) 133-142.
- [2] R. Ragni, F. Scotognella, D. Vona, L. Moretti, E. Altamura, G. Ceccone, D. Mehn, S.R. Cicco, F. Palumbo, G. Lanzani, G.M. Farinola, Hybrid Photonic Nanostructures by In Vivo Incorporation of an Organic Fluorophore into Diatom Algae, *Advanced Functional Materials*, 28 (2018) 1706214.
- [3] F. Daboussi, S. Leduc, A. Maréchal, G. Dubois, V. Guyot, C. Perez-Michaut, A. Amato, A. Falciatore, A. Juillerat, M. Beurdeley, Genome engineering empowers the diatom *Phaeodactylum tricornutum* for biotechnology, *Nature communications*, 5 (2014) 3831.
- [4] H. M. McNair, M. A. Brzezinski, J. W. Krause, Diatom populations in an upwelling environment decrease silica content to avoid growth limitation. *Environmental microbiology*, 20 (2018) 4184-4193.
- [5] Z. Shen, Y. Yao, Y. Wu, Silica supply and diatom blooms in Jiaozhou bay. In: *Studies of the biogeochemistry of typical estuaries and bays in china*. Springer Earth System Sciences, Berlin, Heidelberg. DOI: https://doi.org/10.1007/978-3-662-58169-8_13
- [6] R. Gordon, R.W. Drum, The chemical basis of diatom morphogenesis, in: *International review of cytology*, Elsevier, 1994, pp. 243-372.
- [7] R. Ragni, S.R. Cicco, D. Vona, G.M. Farinola, Multiple routes to smart nanostructured materials from diatom microalgae: a chemical perspective, *Advanced Materials*, 30 (2018) 1704289.

- [8] M. Sumper, E. Brunner, Learning from diatoms: Nature's tools for the production of nanostructured silica, *Advanced Functional Materials*, 16 (2006) 17-26.
- [9] G.L. Rorrer, Chapter 4 functionalization of frustules from diatom cell culture for optoelectronic properties, in: *diatom nanotechnology: Progress and emerging applications*, The Royal Society of Chemistry, 2018, pp. 79-110.
- [10] L. De Stefano, P. Maddalena, L. Moretti, I. Rea, I. Rendina, E. De Tommasi, V. Mocella, M. De Stefano, Nano-biosilica from marine diatoms: A brand new material for photonic applications, *Superlattices and Microstructures*, 46 (2009) 84-89.
- [11] S. Leonardo, B. Prieto-Simón, M. Campàs, Past, present and future of diatoms in biosensing, *TrAC Trends in Analytical Chemistry*, 79 (2016) 276-285.
- [12] L. Ma, F. Wang, Y. Yu, J. Liu, Y. Wu, Cu removal and response mechanisms of periphytic biofilms in a tubular bioreactor, *Bioresource Technology*, 248 (2018) 61-67.
- [13] V. Vinayak, K.B. Joshi, R. Gordon, B. Schoefs, Chapter 3 nanoengineering of diatom surfaces for emerging applications, in: *Diatom nanotechnology: Progress and emerging applications*, The Royal Society of Chemistry, 2018, pp. 55-78.
- [14] M. Diab, T. Mokari, Bioinspired hierarchical porous structures for engineering advanced functional inorganic materials, *Advanced Materials*, 30 (2018) 1706349.
- [15] W. Jiang, S. Luo, P. Liu, X. Deng, Y. Jing, C. Bai, J. Li, Purification of biosilica from living diatoms by a two-step acid cleaning and baking method, *Journal of applied phycology*, 26 (2014) 1511-1518.
- [16] N. Nassif, J. Livage, From diatoms to silica-based biohybrids, *Chemical Society Reviews*, 40 (2011) 849-859.

- [17] C. Jeffryes, J. Campbell, H. Li, J. Jiao, G. Rorrer, The potential of diatom nanobiotechnology for applications in solar cells, batteries, and electroluminescent devices, *Energy & Environmental Science*, 4 (2011) 3930-3941.
- [18] D. Pawolski, C. Heintze, I. Mey, C. Steinem, N. Kröger, Reconstituting the formation of hierarchically porous silica patterns using diatom biomolecules, *Journal of Structural Biology*, 204 (2018) 64-74.
- [19] L.V. Morales, D.M. Sigman, M.G. Horn, R.S. Robinson, Cleaning methods for the isotopic determination of diatombound nitrogen in non-fossil diatom frustules, *Limnology and Oceanography: Methods*, 11 (2013) 101-112.
- [20] J. Romann, M.S. Chauton, S.M. Hanetho, M. Vebner, M. Heldal, C. Thaulow, O. Vadstein, G. Tranell, M.-A. Einarsrud, Diatom frustules as a biomaterial: effects of chemical treatment on organic material removal and mechanical properties in cleaned frustules from two *Coscinodiscus* species, *Journal of Porous Materials*, 23 (2016) 905-910.
- [21] Y. Wang, D. Zhang, J. Cai, J. Pan, M. Chen, A. Li, Y. Jiang, Biosilica structures obtained from *Nitzschia*, *Ditylum*, *Skeletonema*, and *Coscinodiscus* diatom by a filtration-aided acid cleaning method, *Applied microbiology and biotechnology*, 95 (2012) 1165-1178.
- [22] A.B. Bageru, V.C. Srivastava, Biosilica preparation from abundantly available African biomass Teff (*Eragrostis tef*) straw ash by sol-gel method and its characterization, *Biomass Conversion and Biorefinery*, 8 (2018) 971-978.
- [23] M. Dükkancı, Sono-photo-Fenton oxidation of bisphenol-A over a LaFeO_3 perovskite catalyst, *Ultrasonics Sonochemistry*, 40 (2018) 110-116.

- [24] C.-H. Choi, D.-H. Ko, B. Park, Y. Choi, W. Choi, D.-P. Kim, Air-water interfacial fluidic sonolysis in superhydrophobic silicon-nanowire-embedded system for fast water treatment, *Chemical Engineering Journal*, 358 (2019) 1594-1600.
- [25] A.R. Rahmani, A. Mousavi-Tashar, Z. Masoumi, G. Azarian, Integrated advanced oxidation process, sono-Fenton treatment, for mineralization and volume reduction of activated sludge, *Ecotoxicology and Environmental Safety*, 168 (2019) 120-126.
- [26] X. Wu, J. Liu, J.-J. Zhu, Sono-Fenton hybrid process on the inactivation of *Microcystis aeruginosa*: Extracellular and intracellular oxidation, *Ultrasonics Sonochemistry*, 53 (2019) 68-76.
- [27] A. Khataee, B. Kayan, P. Gholami, D. Kalderis, S. Akay, Sonocatalytic degradation of an anthraquinone dye using TiO_2 -biochar nanocomposite, *Ultrasonics Sonochemistry*, 39 (2017) 120-128.
- [28] A. Khataee, P. Gholami, B. Vahid, S.W. Joo, Heterogeneous sono-Fenton process using pyrite nanorods prepared by non-thermal plasma for degradation of an anthraquinone dye, *Ultrasonics Sonochemistry*, 32 (2016) 357-370.
- [29] N.S.M. Yusof, B. Babgi, Y. Alghamdi, M. Aksu, J. Madhavan, M. Ashokkumar, Physical and chemical effects of acoustic cavitation in selected ultrasonic cleaning applications, *Ultrasonics sonochemistry*, 29 (2016) 568-576.
- [30] N. Jaafarzadeh, A. Takdastan, S. Jorfi, F. Ghanbari, M. Ahmadi, G. Barzegar, The performance study on ultrasonic/ $\text{Fe}_3\text{O}_4/\text{H}_2\text{O}_2$ for degradation of azo dye and real textile wastewater treatment, *Journal of Molecular Liquids*, 256 (2018) 462-470.
- [31] X. Li, Y. Zhang, Y. Xie, Y. Zeng, P. Li, T. Xie, Y. Wang, Ultrasonic-enhanced Fenton-like degradation of bisphenol A using a bio-synthesized schwertmannite catalyst, *Journal of Hazardous Materials*, 344 (2018) 689-697.

- [32] N.P. Tantak, S. Chaudhari, Degradation of azo dyes by sequential Fenton's oxidation and aerobic biological treatment, *Journal of Hazardous Materials*, 136 (2006) 698-705.
- [33] A.H. Ltaïef, S. Sabatino, F. Proietto, S. Ammar, A. Gadri, A. Galia, O. Scialdone, Electrochemical treatment of aqueous solutions of organic pollutants by electro-Fenton with natural heterogeneous catalysts under pressure using Ti/IrO₂-Ta₂O₅ or BDD anodes, *Chemosphere*, 202 (2018) 111-118.
- [34] S.G. Babu, P. Aparna, G. Satishkumar, M. Ashokkumar, B. Neppolian, Ultrasound-assisted mineralization of organic contaminants using a recyclable LaFeO₃ and Fe³⁺/persulfate Fenton-like system, *Ultrasonics Sonochemistry*, 34 (2017) 924-930.
- [35] Y. Shen, N. Zhang, Facile synthesis of porous carbons from silica-rich rice husk char for volatile organic compounds (VOCs) sorption, *Bioresource Technology*, 282 (2019) 294-300.
- [36] V.I. Popkov, V.P. Tolstoy, S.O. Omarov, V.N. Nevedomskiy, Enhancement of acidic-basic properties of silica by modification with CeO₂-Fe₂O₃ nanoparticles via successive ionic layer deposition, *Applied Surface Science*, 473 (2019) 313-317.
- [37] Z. Sun, H. Cao, X. Yin, X. Zhang, A. Dong, L. Liu, W. Geng, Precipitation and subsequent preservation of hydrothermal Fe-Mn oxides in distal plume sediments on Juan de Fuca Ridge, *Journal of Marine Systems*, 187 (2018) 128-140.
- [38] A.P. Nowak, M. Sprynsky, W. Brzozowska, A. Lisowska-Oleksiak, Electrochemical behavior of a composite material containing 3D-structured diatom biosilica, *Algal Research*, 41 (2019) 101538.
- [39] Y. Qi, J. Wang, X. Wang, J.J. Cheng, Z. Wen, Selective adsorption of Pb(II) from aqueous solution using porous biosilica extracted from marine diatom biomass: Properties and mechanism, *Applied Surface Science*, 396 (2017) 965-977.

- [40] B. Talluri, T. Thomas, Physicochemical properties of chimie douce derived, digestively ripened, ultra-small ($r < 2$ nm) ZnO QDs, *Colloids and Surfaces A: Physicochemical and Engineering Aspects*, 575 (2019) 310-317.
- [41] L. Wang, S. Zhu, N. Marinkovic, S. Kattel, M. Shao, B. Yang, J.G. Chen, Insight into the synergistic effect between nickel and tungsten carbide for catalyzing urea electrooxidation in alkaline electrolyte, *Applied Catalysis B: Environmental*, 232 (2018) 365-370.
- [42] Y. Yang, W. Wang, M. Li, H. Wang, M. Zhao, C. Wang, Preparation of PANI grafted at the edge of graphene oxide sheets and its adsorption of Pb(II) and methylene blue, *Polymer Composites*, 39 (2018) 1663-1673.
- [43] U. Tyagi, N. Anand, D. Kumar, Simultaneous pretreatment and hydrolysis of hardwood biomass species catalyzed by combination of modified activated carbon and ionic liquid in biphasic system, *Bioresource Technology*, 289 (2019) 121675.
- [44] T. Yoshioka, A. Chávez-Valdez, J. Roether, D. Schubert, A. Boccaccini, AC electrophoretic deposition of organic–inorganic composite coatings, *Journal of colloid and interface science*, 392 (2013) 167-171.
- [45] A. Khataee, A. Fazli, M. Fathinia, F. Vafaei, Removal of diatom *Nitzschia* sp. cells via ozonation process catalyzed by martite nanoparticles, *Journal of Cleaner Production*, 186 (2018) 475-489.
- [46] P. Jiang, Q. Li, C. Gao, J. Lu, Y. Cheng, S. Zhai, Q. An, H. Wang, Fractionation of alkali lignin by organic solvents for biodegradable microsphere through self-assembly, *Bioresource Technology*, 289 (2019) 121640.
- [47] M. Thommes, Physical adsorption characterization of nanoporous materials, *Chemie Ingenieur Technik*, 82 (2010) 1059-1073.

- [48] M. Bertasa, T. Poli, C. Riedo, V. Di Tullio, D. Capitani, N. Proietti, C. Canevali, A. Sansonetti, D. Scalarone, A study of non-bounded/bounded water and water mobility in different agar gels, *Microchemical Journal*, 139 (2018) 306-314.
- [49] E. Van Eynde, B. Lenaerts, T. Tytgat, S.W. Verbruggen, B. Hauchecorne, R. Blust, S. Lenaerts, Effect of pretreatment and temperature on the properties of *Pinnularia biosilica* frustules, *RSC Advances*, 4 (2014) 56200-56206.
- [50] A. Goudie, The chemistry of world calcrete deposits, *The Journal of Geology*, 80 (1972) 449-463.
- [51] Q. Li, J. Zhang, Q. Lu, J. Lu, J. Li, C. Dong, Q. Zhu, Hydrothermal synthesis and characterization of ordered mesoporous magnesium silicate-silica for dyes adsorption, *Materials Letters*, 170 (2016) 167-170.
- [52] C. X. Gui, Q. Q. Wang, S. M. Hao, J. Qu, P. P. Huang, C. Y. Cao, W. G. Song, Z. Z. Yu, Sandwichlike magnesium silicate/reduced graphene oxide nanocomposite for enhanced Pb^{2+} and methylene blue adsorption, *ACS applied materials & interfaces*, 6 (2014) 14653-14659.

Figure captions

Fig. 1. (a) Comparative evaluation of performance of different processes in TOC and TN removal from diatom cells; (b) the effect of scavengers on TOC and TN removal efficiencies through US, Fenton and SF processes (pH = 3, diatom cell density = 4.8×10^5 cell mL⁻¹, [H₂O₂]₀ = 60 mM, [Fe²⁺]₀ = 15 mM, ultrasound irradiation power = 400 W, temperature = 25 °C, reaction time = 240 min and [scavenger] = 0.2 M); Note: RE% refers to removal efficiency.

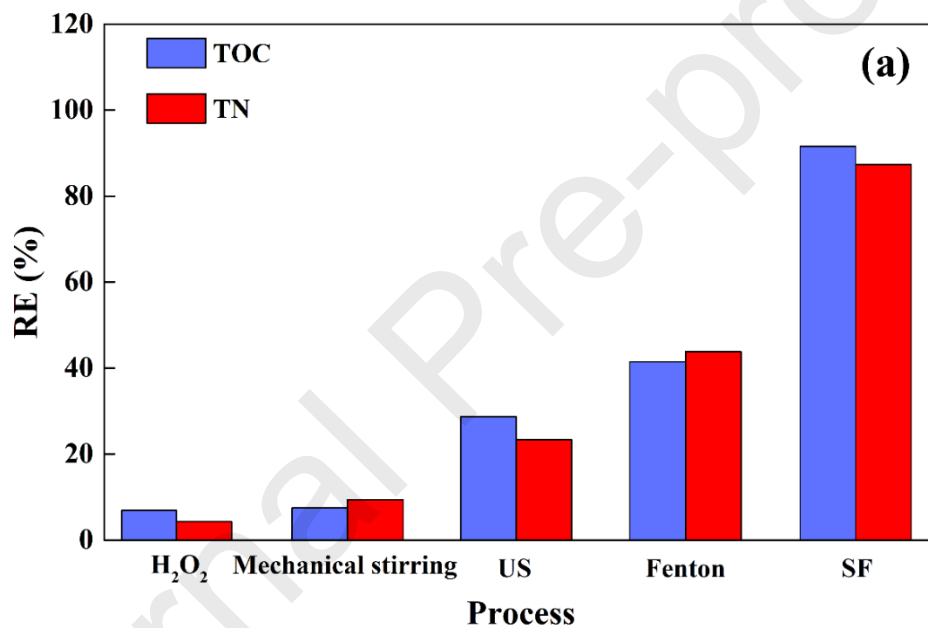
Fig. 2. Effect of (a) suspension pH (pH = 3, diatom cell density = 4.8×10^5 cell mL⁻¹, [H₂O₂]₀ = 40 mM, [Fe²⁺]₀ = 5 mM, ultrasound irradiation power = 400 W, temperature = 25 °C and reaction time = 240 min), (b) H₂O₂ concentration (pH = 3, diatom cell density = 4.8×10^5 cell mL⁻¹, [Fe²⁺]₀ = 5 mM, ultrasound irradiation power = 400 W, temperature = 25 °C and reaction time = 240 min), (c) Fe²⁺ concentration (pH = 3, diatom cell density = 4.8×10^5 cell mL⁻¹, [H₂O₂]₀ = 60 mM, ultrasound irradiation power = 400 W, temperature = 25 °C and reaction time = 240 min), (d) diatom cell density (pH = 3, diatom cell density = 4.8×10^5 cell mL⁻¹, [H₂O₂]₀ = 60 mM, [Fe²⁺]₀ = 15 mM, ultrasound irradiation power = 400 W, temperature = 25 °C and reaction time = 240 min), (e) ultrasound irradiation power (pH = 3, diatom cell density = 4.8×10^5 cell mL⁻¹, [H₂O₂]₀ = 60 mM, [Fe²⁺]₀ = 15 mM, temperature = 25 °C and reaction time = 240 min), and (f) temperature (pH = 3, diatom cell density = 4.8×10^5 cell mL⁻¹, [H₂O₂]₀ = 60 mM, [Fe²⁺]₀ = 15 mM, ultrasound irradiation power = 400 W and reaction time = 240 min); Note: RE% refers to removal efficiency.

Fig. 3. SEM micrographs of UF (a and b) and TF (c and d); EDX spectra of UF (e) and TF (f).

Fig. 4. XRD patterns (a), FT-IR spectra (b), N₂ adsorption-desorption isotherms (c) and TGA spectra of UF and TF samples.

Fig. 5. Comparison of adsorption capacities of UF and TF for removal of MB (pH = 5.6, [MB]₀ = 50 mg L⁻¹, amount of adsorbent = 0.02 g and temperature = 25 °C).

Figures



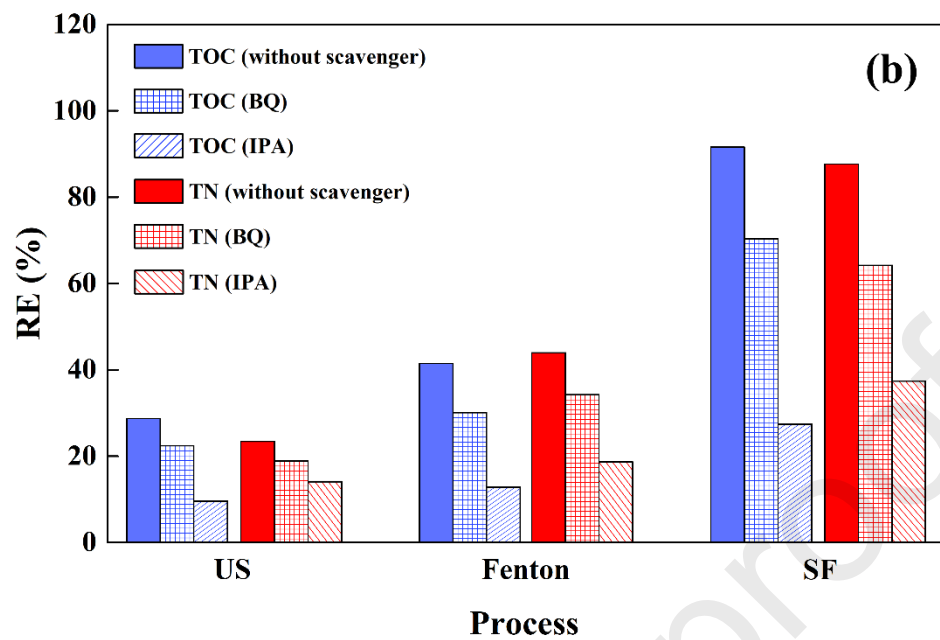


Fig. 1

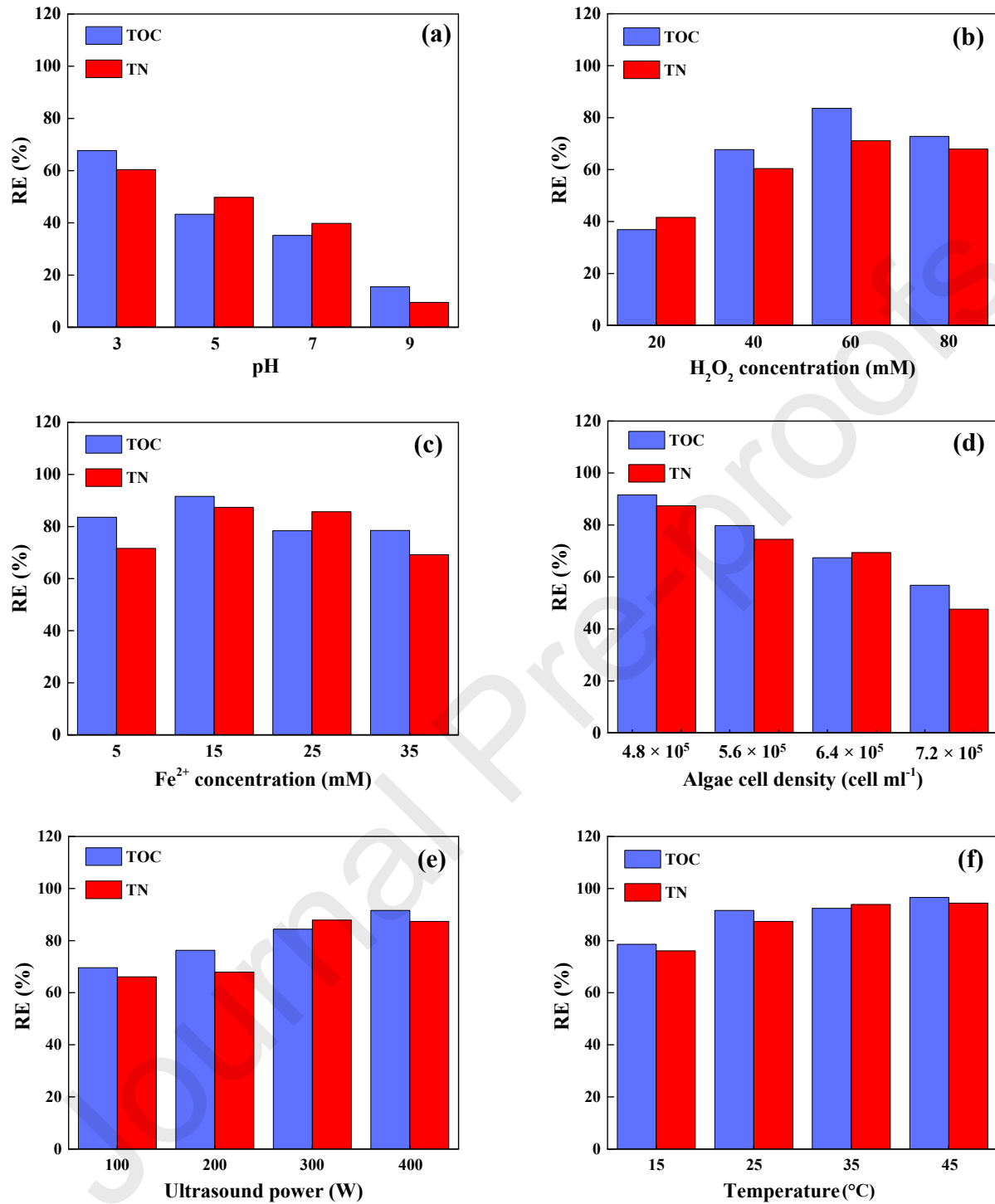


Fig. 2

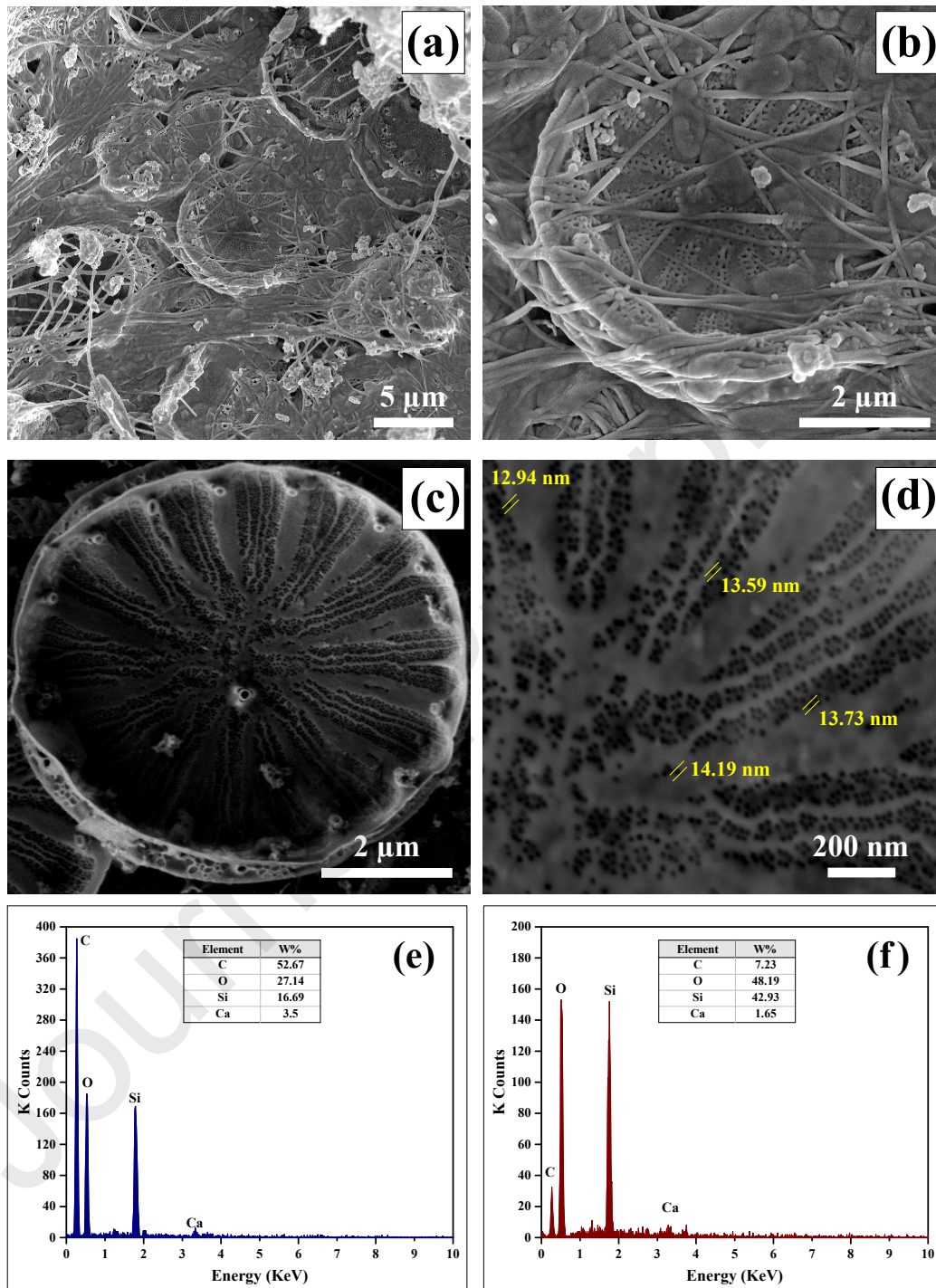


Fig. 3

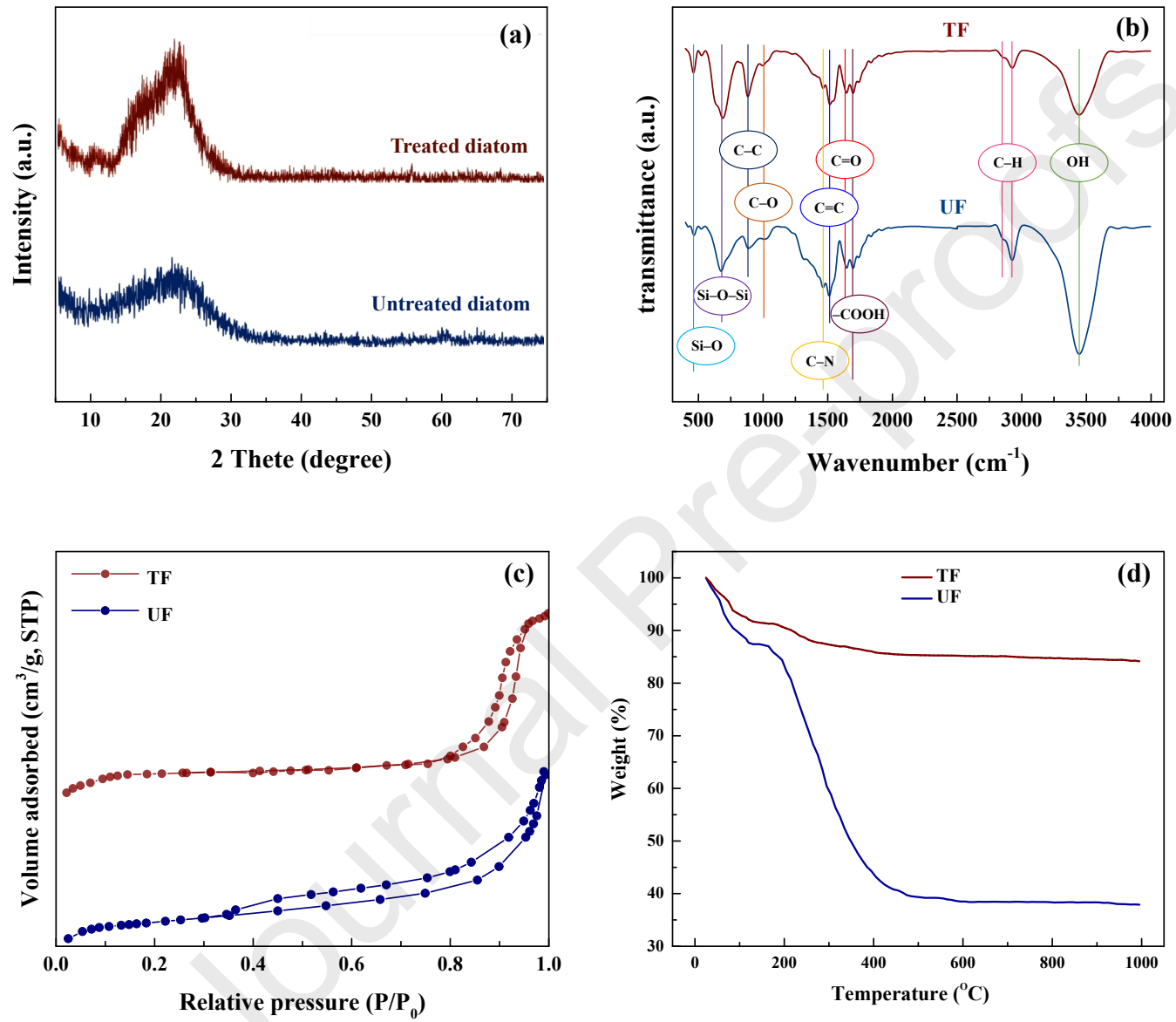


Fig. 4

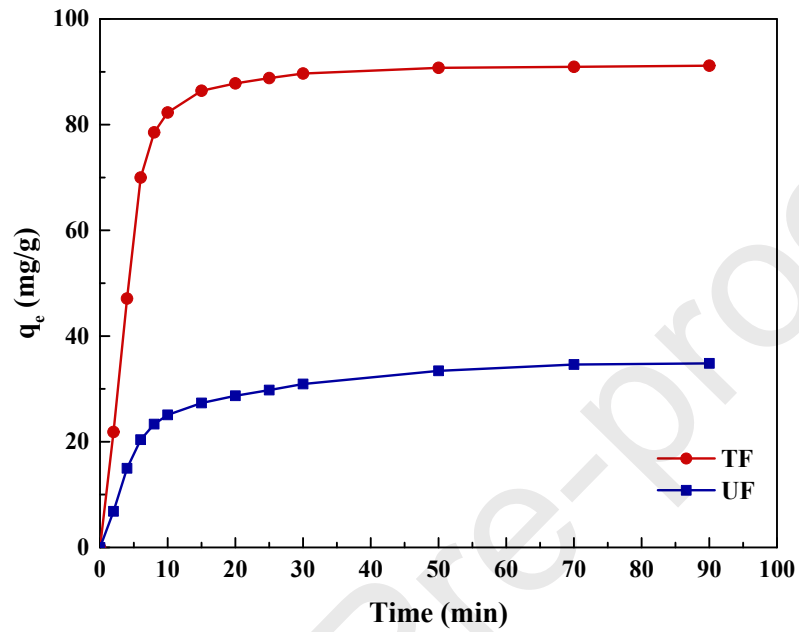


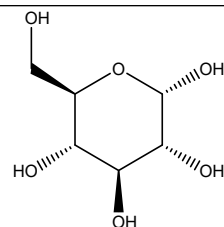
Fig. 5

Tables

Table 1. Identified organic compounds during SF treatment of diatom cells.

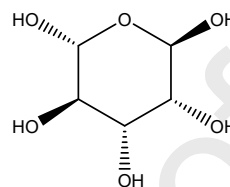
No.	Compound name	Structure	Retention time (min)

1 (2S,3R,4S,5S,6R)-6-(hydroxymethyl)oxane-2,3,4,5-tetrol



31.602

2 (2R,3R,4R,5R,6S)-6-methyloxane-2,3,4,5-tetrol



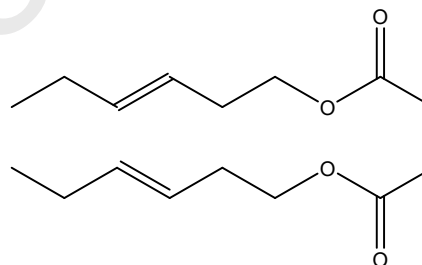
30.183

3 (Z)-hexadec-9-enoic acid



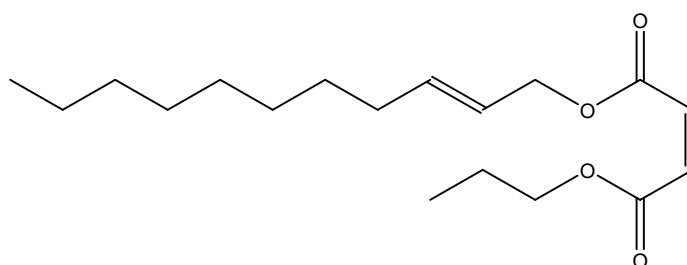
25.610

4 bis[(E)-hex-3-enyl] (E)-but-2-enedioate



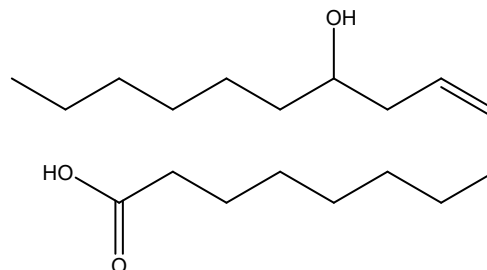
27.386

5 1-O-propyl 4-O-[(E)-undec-2-enyl] (E)-but-2-enedioate

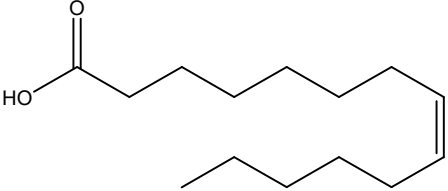
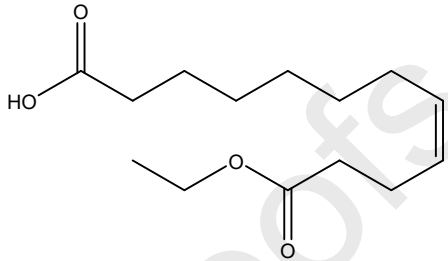
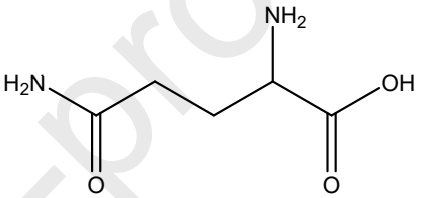
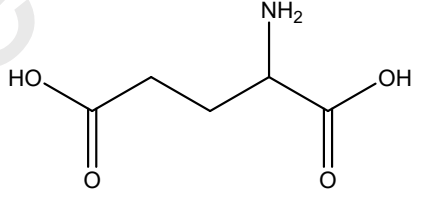
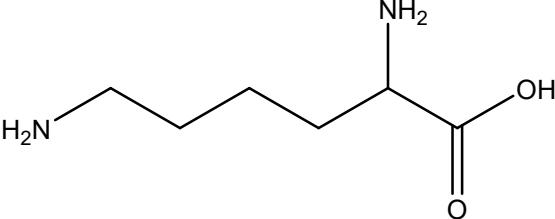
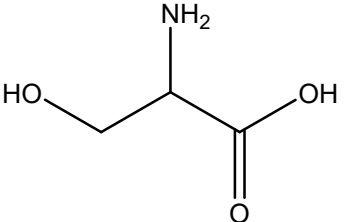


29.537

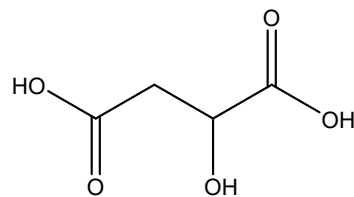
6 12-hydroxyoctadec-9-enoic acid



28.394

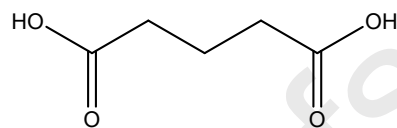
7	(Z)-tetradec-7-enoic acid		21.553
8	Ethyl 12-oxododecanoate		23.943
9	(2S)-2,5-diamino-5-oxopentanoic acid		16.841
10	(2R)-2-aminopentanedioic acid		14.283
11	(2S)-2,6-diaminohexanoic acid		16.271
12	(2S)-2-amino-3-hydroxypropanoic acid		9.192

13 (7R,11R)-3,7,11,15-tetramethylhexadecanoic acid



6.617

14 Pentanedioic acid

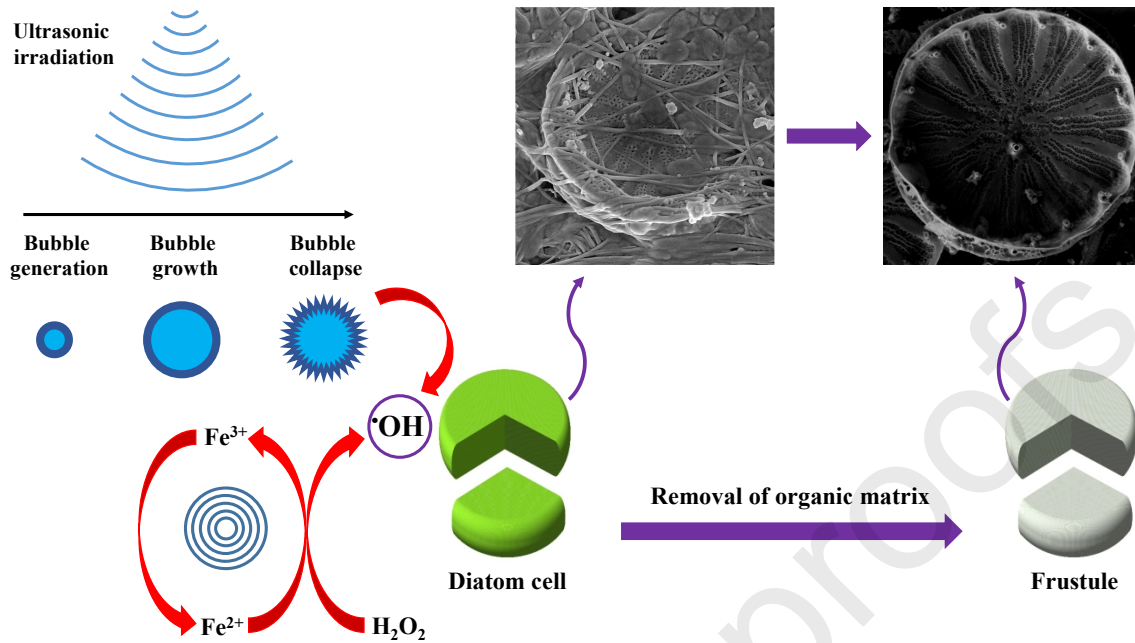


8.960

Highlights

- Removal of organic materials from diatom frustules using sono-Fenton process
- Characterization of the obtained nanoporous silica by SEM, XRD, FT-IR, BET and TGA
- Study of the effect of operational parameters on the cleaning of diatom frustules
- Identification of the organic compounds released from diatom cells to the solution

Graphical Abstract



Cleaning of diatom frustules using Sono-Fenton process

Declaration of Interest Statement

We would like to confirm that there is no known conflict of interest associated with this publication.